RSC Advances

PAPER

View Article Online
View Journal | View Issue

Cite this: *RSC Adv.*, 2023, **13**, 23043

New insights into the process of intrinsic point defects in PuO_2

Huilong Yu,† Shuaipeng Wang,† Ruizhi Qiu, Gan Li, Haibo Li, Xin Xiang and Wenhua Luo*

Intrinsic point defects are known to play a crucial role in determining the physical properties of solid-state materials. In this study, we systematically investigate the intrinsic point defects, including vacancies (V_{Pu} and V_O), interstitials (Pu_i and O_i), and antisite atoms (Pu_O and O_{Pu}) in PuO_2 using the first-principles plane wave pseudopotential method. Our calculations consider the whole charge state of these point defects, as well as the effect of oxygen partial pressure. This leads to a new perspective on the process of intrinsic point defects in PuO_2. We find that the antisite atoms O_{Pu} and Pu_O are more likely to appear in O-rich and O-deficient environments, respectively. Interestingly, the most energetically favorable type of Schottky defect is $\{2V_{Pu}^{3-}: 3V_O^{2+}\}$ in an O-rich environment, while $\{4V_O^{1+}: V_{Pu}^{4-}\}$ is preferred in an O-deficient environment. These results differ from the commonly known $\{V_{Pu}^{4-}: 2V_O^{2+}\}$ type of Schottky defect. Moreover, under O-deficient conditions, we predict that the stable cation Frenkel defect is $\{V_{Pu}^{4+}: Pu_i^{4+}\}$, while the most stable anion Frenkel defect is $\{V_O^{2+}: O_i^{2-}\}$ under O-rich conditions. Lastly, we find that the only two types of antisite pairs that can appear are $\{O_{Pu}^{5-}: Pu_O^{5+}\}$ and $\{O_{Pu}^{6-}: Pu_O^{6+}\}$, with the latter being the more stable configuration. These unconventional defect configurations provide a new viewpoint on the process of intrinsic point defects in PuO_2 and lay theoretical foundations for future experiments.

Received 27th June 2023
Accepted 25th July 2023

DOI: 10.1039/d3ra04306a

rsc.li/rsc-advances

1 Introduction

The study of plutonium oxides has attracted significant attention from scientists due to their critical role in the permanent storage of Pu-based radioactive waste and the nuclear fuel cycle.[1–6] Their complex chemical reactions and impressive physical properties have also contributed to their importance. Many researchers have investigated various physical and chemical properties of PuO_2 because it is considered the standard in plutonium reuse, separation, and permanent storage.[7–11] The redox properties of Pu-oxides are crucial to plutonium science and reactor safety because different oxidation states lead to different solubility levels, which can impact the chemical corrosion of the plutonium surface.[3–6] This topic has been explored extensively by researchers, as highlighted in several studies.[1–11]

There has been considerable research interest in stoichiometric PuO_2; however, studies on non-stoichiometric PuO_2 remain inadequate.[1,8] In reality, under various external environments, PuO_2 with a fluorite structure is non-stoichiometric.[10,12,13] The stoichiometry of PuO_2 is known to have a significant impact on important physical properties like lattice parameters, thermodynamical stability, and melting temperature.[14] Therefore, it is essential to investigate the characteristics of defects in non-stoichiometric PuO_2 composition to understand the variation in its physical properties.

Direct measurement of formation energies and defect concentrations for non-stoichiometric PuO_2 is challenging and intricate.[8] As a result, theoretical models have been developed in the defect properties of PuO_2. However, conventional DFT that applies the local density approximation (LDA) or generalized gradient approximation (GGA), proves failure in accounting for the strong correlation of 5f electrons, describing PuO_2 as an incorrect ferromagnetic (FM) conductor.[8,15,16] Nonetheless, correction schemes such as self-interaction correction (SIC), DFT+U, and hybrid functional have been implemented to mitigate the inefficiencies associated with conventional DFT in PuO_2.[16,17]

Nowadays research on point defects in PuO_2 primarily focus on only four types of isolated point defects interstitial (Pu_i, O_i) and vacancies (V_{Pu}, V_O) in PuO_2, which are described with their full formal charges state: Pu_i^{4+}, O_i^{2-}, V_{Pu}^{4-}, and V_O^{2+}.[1] Antisite defects such as O_{Pu} and Pu_O rarely come into play due to their high formation energy in metallic oxide, although conclusive evidence regarding their role in PuO_2 is lacking.[18,19] M. Freyss has suggested that oxygen Frenkel pair formation is more difficult than Schottky defect formation, and that the plutonium Frenkel pair defect have lower formation energy

Institute of Materials, China Academy of Engineering Physics, Mianyang, 621907, China. E-mail: luowenhua@caep.cn

† These authors contribute equally to this work.

compared to Schottky defects.[7] However, charge-neutral combinations of anion and cation with full formal charge states (*e.g.*, $V_{Pu}^{4-} + 2V_O^{2+}$ for Schottky defects, $V_O^{2+} + O_i^{2-}$ for oxygen Frenkel pairs, and $V_{Pu}^{4-} + O_i^{4+}$ for plutonium Frenkel pairs) are artificially assumed to be sources of intrinsic point defects during the defect formation process.[21,22] In reality, the charge state of intrinsic point defects changes with oxygen potential and Fermi energy, and the equilibrium charge state for V_O is neutral.

The insufficient understanding of the defect process in PuO_2 has encouraged us to conduct a comprehensive analysis of its innate point defects. We have employed the first-principles plane-wave pseudopotential method to investigate the charge states and formation energies of these defects, along with their variation with oxygen partial pressure in PuO_2. Therefore, this work will constitute a benchmark for future experimental or theoretical studies.

2 Computational method and model

Total energy calculations are carried out with VASP code, which employs the project augmented-wave (PAW) method and generalized gradient approximation (GGA) functional.[23] To account for strong correlations, the Hubbard model was used with the DFT+U method, incorporating values of $U = 4.75$ eV and $J = 0.75$ eV for 5f electrons of Pu.[1] These values are tested and the qualitative conclusion in this work is not affected by the choice of U and J. A $2 \times 2 \times 2$ supercell, consisting of 32 plutonium atoms and 64 oxygen atoms, was constructed to create the defect model. Brillouin zone integrations were performed using a $3 \times 3 \times 3$ k-point mesh. The electron wave function was expanded in plane waves up to a cutoff energy of 500 eV, which is sufficient to ensure that errors in intrinsic point defect formation energies are less than 1 meV.

In this study, shown in Fig. 1, six types of point defects are considered. These include interstitial (O_i, Pu_i), vacancy (V_O, V_{Pu}), and antisite atom (O_{Pu}, Pu_O) defects that are created by introducing, removing, or substituting a corresponding atom in the PuO_2 supercell. Four typical intrinsic point defect processes of forming plutonium Frenkel, oxygen Frenkel, Schottky defects, and antisite pairs defect are examined. Charge-neutral conditions are imposed for defects in pure PuO_2 bulk. A Frenkel pair is composed of a vacancy and a corresponding interstitial atom ($O_i + V_O$, $Pu_i + V_{Pu}$), while a Schottky defect comprises several vacancy defects ($mV_{Pu} + nV_O$). On the other hand, the antisite pair defect consists of two types of antisite atoms (O_{Pu} and Pu_O) separated by different distances.

The formation energy $\Delta E^f_{def}(X, q)$ of intrinsic point defect X in charge state q is given by the following equation: [23]

$$\Delta E^f_{def}(X,q) = E^{tot}_{def} - E^{tot}_{perf} + \sum_i \Delta n_i \mu_i + qE_F, \quad (1)$$

where E^{tot}_{def} and E^{tot}_{perf} are the total energy of defective X supercell and perfect supercell, respectively. Here E_F is the Fermi energy and its value varies from zero to the width of the band gap in the perfect crystal, *i.e.*, 2.85 eV.[10,20] For each defect species, the charge state q varies from neutral to fully ionized states, such as 0–+2 for V_O, −4–0 for V_{Pu}, −2–0 for O_i, 0–+4 for Pu_i, −6–0 for O_{Pu}, and 0–+6 for Pu_O. The symbol Δn_i is the number of atom species i removed (positive) or added (negative), and $\Delta\mu_i$ is the chemical potential of atom i with a positive (negative) symbol for interstitial (vacancy) defect. The reference chemical potential for Pu and O atoms are chosen as that of δ-Pu and molecular O_2, respectively.

According to the thermodynamic equilibrium condition, the heat of formation must be equal to the sum of the chemical potentials of atoms in PuO_2 to ensure the stability of the compound PuO_2. The equation condition can be expressed as

$$\mu_{PuO_2} = \mu_{Pu} + 2\mu_O \quad (2)$$

where μ_{PuO_2} is the chemical potential of PuO_2 per formula unit. However, the atomic chemical potentials are determined by the experiment such as temperature, pressure, and oxygen potential, and we can use the well-known thermodynamic expression:[24,25]

$$\mu_O(T, p_{O_2}) = \frac{1}{2}\left(E_{O_2} + \mu_{O_2}(T, p^0) + k_B T \ln\left(\frac{p_{O_2}}{p^0}\right)\right) \quad (3)$$

where E_{O_2} is the total energy of an oxygen molecule. For the standard pressure $p^0 = 1$ atm, the values of $\mu_{O_2}(T, p^0)$ consult the reference. Within the "*ab initio* atomic thermodynamics" method, the total energies are provided by the DFT+U calculations. The environmental dependence of $\Delta E^f_{def}(X,q)$ is determined by μ_O, which is affected by the three key factors (T, p_{O_2}, and μ_{O_2}).

Thus, two extreme conditions of O-rich and O-deficient are taken into account here, as the condition of PuO_2 is relative temperature and pressure fixed. Under O-rich condition, μ_O and μ_{Pu} are determined by the total energy of an oxygen molecule, *i.e.*, $\mu_O = \mu_{O_2}/2$, $\mu_{Pu} = \mu_{PuO_2} - 2\,\mu_O$. While in O-deficient environment, μ_O and μ_{Pu} are determined by the total energy of the α-Pu unit cell, *i.e.*, $\mu_{Pu} = \mu^{metal}_{Pu}$, $\mu_O = (\mu_{PuO_2} - \mu_{Pu})/2$.

3 Results and discussion

3.1 Isolated intrinsic point defect

The formation energies of six types of isolated intrinsic point defects (Pu_O, O_{Pu}, O_i, Pu_i, V_{Pu}, and V_O) as a function of the Fermi level E_F according to eqn (1) are presented in Fig. 2, under O-rich and O-deficient conditions. Only the energetically favourable charge states are labelled in Fig. 2 for clarity. It is important to note that this study represents the first investigation of two types of antisite point defects (O_{Pu} and Pu_O). The formation energies of Pu_O under O-deficient conditions and O_{Pu} under O-rich conditions are significantly negative and the smallest within some range of E_F. This indicates that O_{Pu} and Pu_O would likely be formed under O-rich and O-deficient conditions, respectively. Therefore, when investigating defect properties in PuO_2, it is critical to consider the antisite atom Pu_O and O_{Pu}.

From Fig. 2a, it can be concluded that plutonium-related defects tend to have higher formation energies than oxygen-related defects under O-rich condition. Conversely, as shown in Fig. 2b, oxygen-related defects have higher formation

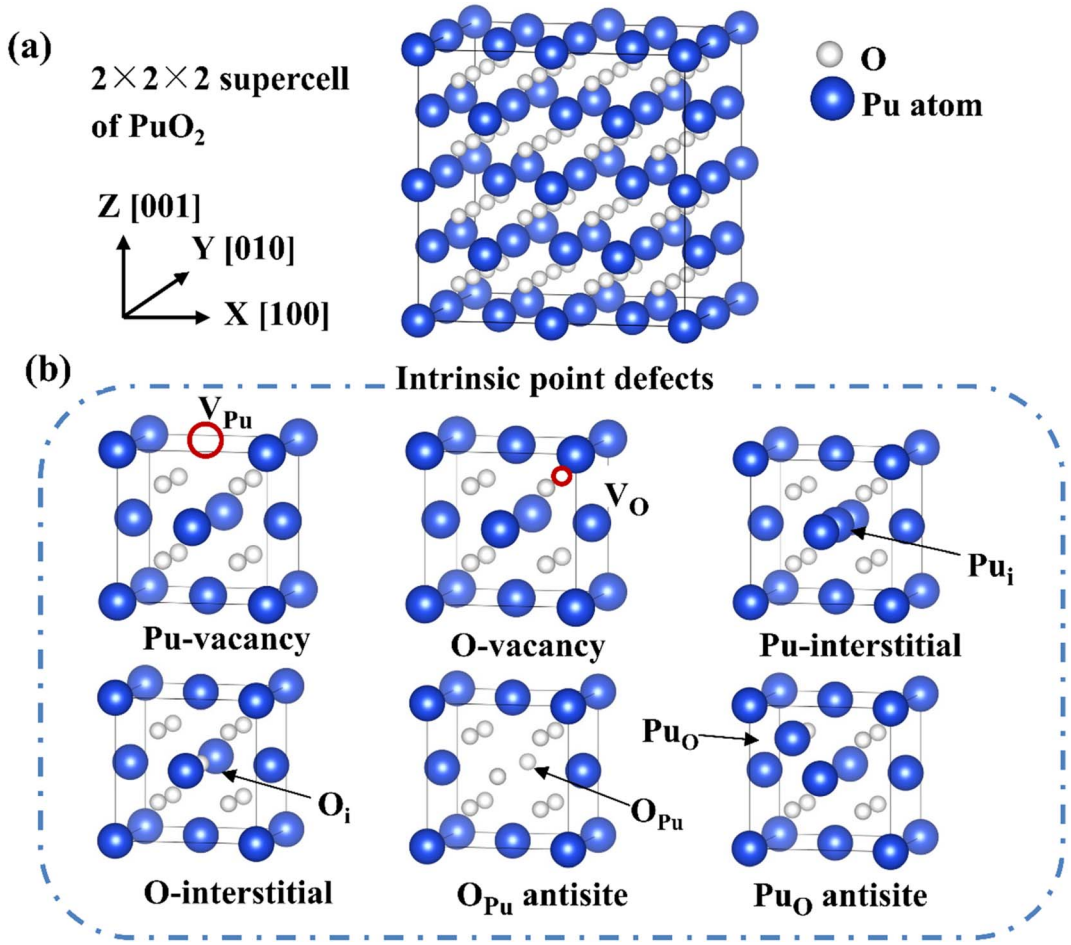

Fig. 1 (a) The 2 × 2 × 2 supercell of PuO_2. (b) The description of six types isolated intrinsic point defect in the PuO_2 unit cell.

energies than plutonium-related defects under O-deficient condition. Additionally, in both O-rich and O-deficient environments, the most stable state charge for each defect species varies with the Fermi level. Specifically, when E_F is located near the top of the valence band under O-rich condition, intrinsic point defect species are ranked in order of rising sequence of formation energies: V_{Pu}^{4-}, V_O^{2+}, O_{Pu}^{6-}, Pu_i^{4+}, O_i^{2-}, and Pu_O^{6+}. When E_F is positioned near the bottom of the conduction band under O-rich conditions, the ranking changes to O_{Pu}^{6-},V_{Pu}^{4-}, O_i^{2-}, V_O^{2+}, Pu_i^{3+}, and Pu_O^{2+}. Under the O-deficient condition, when E_F locate near the top of valence band, the ranking changes to Pu_O^{6+}, V_O^{2+}, Pu_i^{4+}, V_{Pu}^{4-}, O_i^{2-}, and O_{Pu}^{3-}. When E_F position is near the bottom of the conduction band under O-deficient condition, the ranking changes to V_{Pu}^{4-}, V_O^{2+}, Pu_O^{2+}, Pu_i^{3+}, O_{Pu}^{5-}, and O_i^{2-}.

The presence of V_{Pu}^{4-} and O_{Pu}^{6-} are strong indications for the existence of $PuO_{2\pm x}$ under certain environmental condition.[8] Previous research has ignored the intrinsic point defects of antisite atoms O_{Pu} and Pu_O, failing to provide convincible evidence. However, this study shows that V_{Pu}^{4-} and O_{Pu}^{6-} are the dominant defect configurations under O-rich conditions, while V_O^{2+} and Pu_O^{6+} dominate under O-deficient conditions. These results suggest that antisite atoms are the dominant intrinsic defects in both scenarios. Specifically, under O-rich conditions, adding oxygen atoms to existing Pu vacancies is more favourable than adding them interstitially, as indicated by the lower formation energy of O_{Pu}^{6-} compared to O_i^{2-}. Conversely, under O-deficient conditions, V_O^{2+} accounts for the lowest formation energy at mostly Fermi level. The most favourable structure for interstitial atom Pu_i varies from +4 to +3, thus explaining why Pu_O commonly has a charge of +6 or +5 near the valence band, as it forms *via* adding a Pu atom to the existing O vacancy. It is also noteworthy that the formation energies of Pu_O and Pu_i under O-rich conditions, and O_i and O_{Pu} under deficient conditions are too high to form in PuO_2 at the equilibrium state, hence qualifying as minor defects.

3.2 Schottky defect

The Schottky defect in PuO_2 is a combination of cation and anion defects, often artificially considered to be of triplet (V_{Pu}^{4+} + $2V_O^{2-}$), given that PuO_2 is an ionic compound of Pu^{4+}: O^{2-}. In this study, we present the formation energies of various Schottky defects with respect to the Fermi energy, as shown in Fig. 3. Our results indicate that the main stable charge states for V_{Pu} are +3 and +4 throughout the range of the Fermi level of PuO_2. While the most stable state for V_O is not +1, the formation

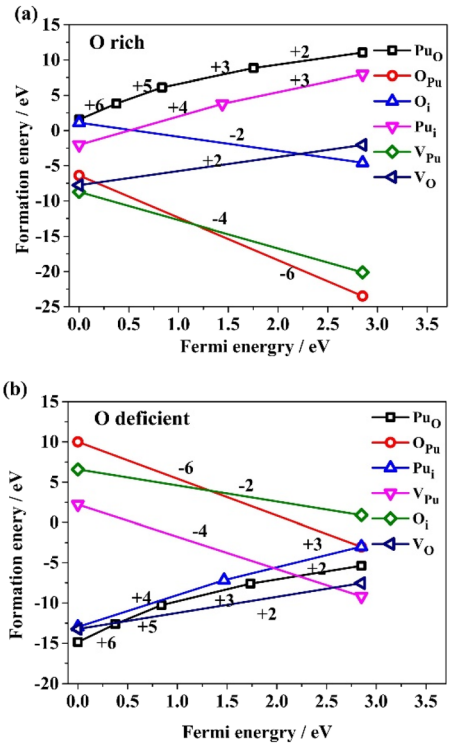

Fig. 2 The formation energies correspond to the most favourable charge state of the isolated intrinsic point defects (Pu_O, O_{Pu}, O_i, Pu_i, V_{Pu} and V_O) under conditions of O-rich (a) and O-deficient (b), *versus* Fermi energy E_F.

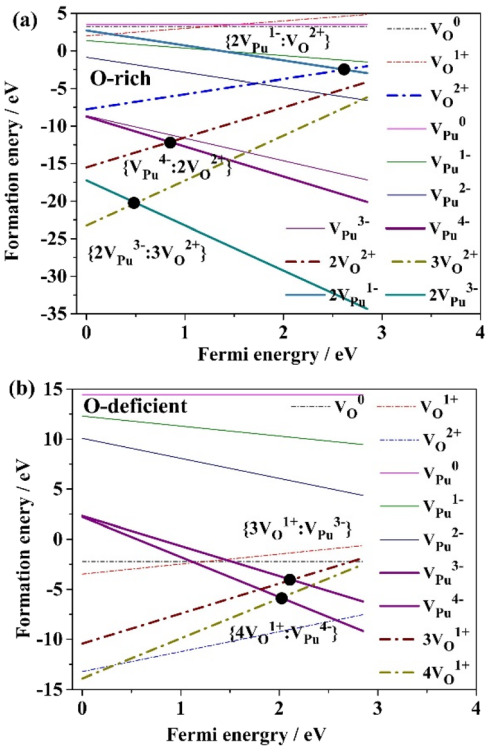

Fig. 3 Formation energies of oxygen vacancies and plutonium vacancies in various charge states within whole E_F level, and possible Schottky defect combination formed in PuO_2 under the conditions of (a) O-rich, (b) O-deficient.

energy of V_O^{+} is lower than zero under O-deficient conditions, suggesting that it is stable. Although Schottky defects in PuO_2 could consist of several ion compounds besides $(V_{Pu}^{4+} + 2V_O^{2-})$, we calculated the formation energies of other combinations, including $(2V_{Pu}^{3+} + 3V_O^{2-})$ and $(4V_O^{+} + V_{Pu}^{4-})$. The results indicate that the formation energies of these combinations are much too high, implying that the vacancy defects should be spaced far enough apart from each other to form a Schottky defect. In fact, under extreme conditions, the space between vacancies could be so great that their interactions become infinitely small. Furthermore, the average formation energy of each component must have an equal value for a Schottky defect to form.

The point of intersection Fig. 3 represents a possible Schottky defect in PuO_2. Two cases of Schottky defects are shown in Fig. 3a and b. All cases are obtained by enumeration. When exposed to O-rich conditions, as seen in Fig. 3a, the average formation energies of three possible Schottky defects $\{2V_{Pu}^{3-}: 3V_O^{2+}\}$, $\{V_{Pu}^{4-}: 2V_O^{2+}\}$, and $\{2V_{Pu}^{1-}: V_O^{2+}\}$ are −20.26 eV, −12.10 eV, and −2.44 eV, respectively. According to the thermodynamic theory, the primary Schottky defect is $\{2V_{Pu}^{3-}: 3V_O^{2+}\}$ due to its lowest formation energy, rather than $\{V_{Pu}^{4-}: 2V_O^{2+}\}$, which was customarily considered as the primary defect under O-rich conditions. This finding provides a fresh perspective on Schottky defects in PuO_2. Further, $\{2V_{Pu}^{1-}: V_O^{2+}\}$ acts as a minor Schottky defect; its formation energy is significantly higher than that of the other defects.

Under O-deficient condition, the average formation energies of $\{4V_O^{1+}: V_{Pu}^{4+}\}$ and $\{3V_O^{1+}: V_{Pu}^{3-}\}$ are −5.75 eV and −4.01 eV, respectively, as shown in Fig. 3b. Interestingly, the V_O charge state of +1 is not the most stable for V_O. The main Schottky defect is $\{4V_O^{1+}: V_{Pu}^{4-}\}$, which has the lowest formation energy under O-deficient conditions, despite not being consistent with the commonly considered $\{V_{Pu}^{4-}: 2V_O^{1+}\}$. However, the small formation energy difference between these two types of Schottky defects indicates that neither will dominate in PuO_2.

When comparing an O-deficient condition and an O-rich condition, the average formation energies of the prominent Schottky defect species ($\{2V_{Pu}^{3-}: 3V_O^{2+}\}$ and $\{V_{Pu}^{4-}: 2V_O^{2+}\}$) are significantly lower in the O-rich environment. This suggests that it is much easier to form dominant Schottky defect species in an O-rich condition. Notably, the Schottky defect species differ entirely between O-rich and O-deficient conditions, indicating that the formation of Schottky defects is dependent on oxygen partial pressure. These results agree with earlier findings.[8]

3.3 Frenkel defect

The Frenkel defect in PuO_2 comprises of an anion Frenkel $\{O_i: V_O\}$ and a cation Frenkel $\{Pu_i: V_{Pu}\}$, whose charge states are commonly considered as $\{O_i^{2-}: V_O^{2+}\}$ and $\{Pu_i^{4+}: V_{Pu}^{4-}\}$. However, just like described in Section 3.2 for the charge states of V_{Pu} (+3 and +4), the custom standpoint for the cation Frenkel defect may differ. To further investigate this, the relative energy

of the PuO_2 supercell was calculated, which includes Frenkel defects ($\{O_i: V_O\}$ and $\{Pu_i: V_{Pu}\}$) at different separation distances between a vacancy and corresponding interstitial atom. Fig. 4 presents the structural model of the Frenkel defect in the 2 × 2 × 2 supercell of PuO_2, where the separation distance between the interstitial atom and vacancy is 1NN (the nearest neighbour). In addition, Fig. 5 illustrates the relative energies of the Frenkel defect for varying separation distances between the vacancy and interstitial atom. The outcome suggests that the relative energies of the Frenkel defect decrease as the distance increases, indicating that the most stable configuration happens when the cation Frenkel defect has an interstitial atom Pu_i closest to the vacancy V_{Pu} (1 NN). The stability behaviour of the anion Frenkel defect is consistent with that of the cation Frenkel defect. It's noteworthy that Frenkel defects differ significantly from Schottky defects, whose stability increases as the V_{Pu} vacancy moves away from the V_O vacancy.

The formation energies of possible plutonium Frenkel defects have been calculated under both O-rich and O-deficient conditions, as shown in Fig. 6. It is worth noting that under O-rich conditions, no plutonium Frenkel defect can form. Conversely, under O-deficient conditions, two types of plutonium Frenkel defects, *i.e.*, $\{V_{Pu}^{3-}: Pu_i^{3+}\}$ and $\{V_{Pu}^{4+}: Pu_i^{4+}\}$, are formed with formation energies of −4.52 eV and −5.35 eV, respectively. Intriguingly, the difference in formation energy between the two types of defects is minimal (<1 eV), suggesting that a significant proportion of $\{V_{Pu}^{3-}: Pu_i^{3+}\}$ may also form in PuO_2, besides $\{V_{Pu}^{4+}: Pu_i^{4+}\}$. This provides a new perspective on oxygen Frenkel defects under O-deficient condition.

The possible oxygen Frenkel defects' formation energies under both O-rich and O-deficient conditions are presented in Fig. 7. Notably, no plutonium Frenkel defect is formed under O-rich conditions, which deviates from typical expectations. However, two types of oxygen Frenkel defects, *i.e.*, $\{V_O^{+}: O_i^{-}\}$ and $\{V_O^{2+}: O_i^{2-}\}$, do form under O-deficient condition, and their respective formation energies are 2.17 eV and −3.30 eV. Of these two defects, the $\{V_O^{2+}: O_i^{2-}\}$ variant is the more prevalent oxygen Frenkel defect due to its lower average formation energy. Conversely, the formation energy of 2.17 eV for the Frenkel defect $\{V_O^{+}: O_i^{-}\}$ is too large to emerge under O-deficient condition.

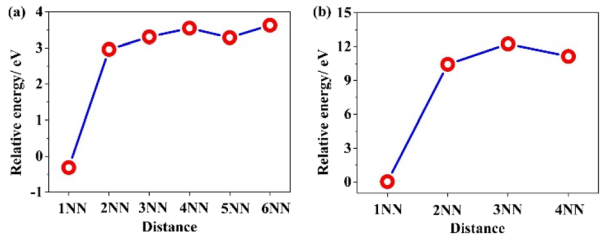

Fig. 5 Relative energies of the (2 × 2 × 2) PuO_2 supercell including (a) oxygen and (b) plutonium Frenkel defect as a function of separate distance between corresponding vacancy and interstitial atom.

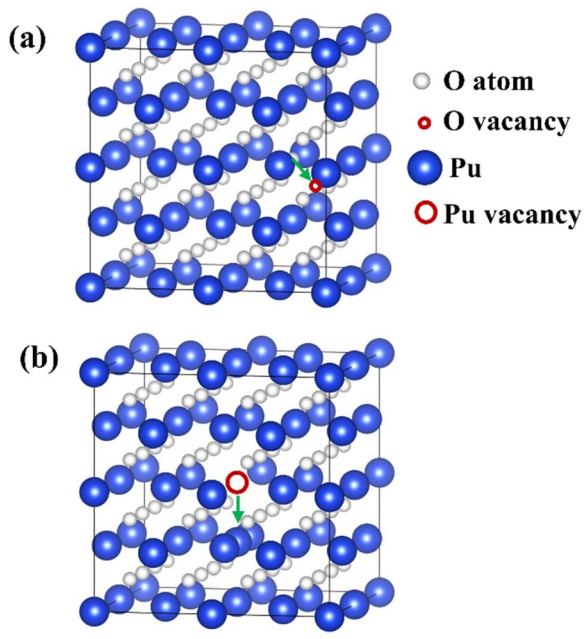

Fig. 4 The structural models of (a) anion and (b) cation Frenkel defects in the 2 × 2 × 2 supercell of PuO_2, when the space distance between vacancy atoms is the nearest neighbour.

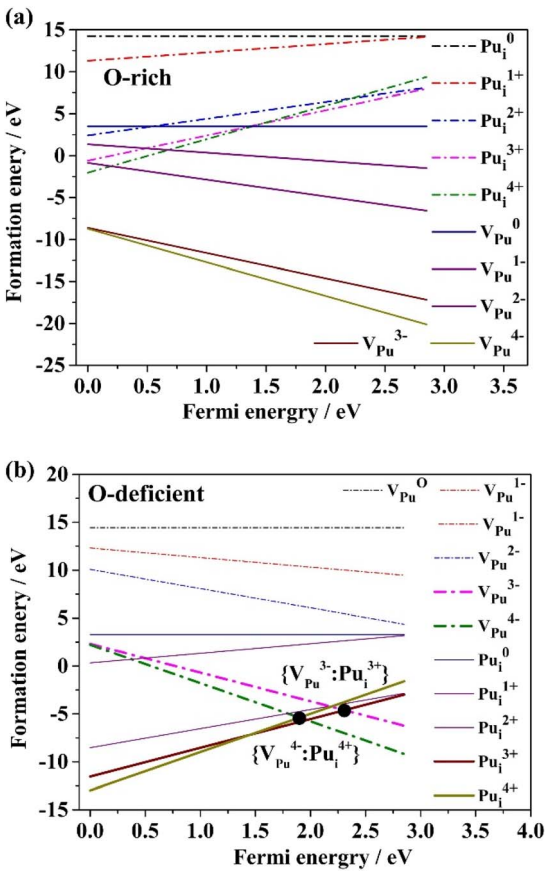

Fig. 6 Formation energies of plutonium vacancies in various charge states within whole E_F level, and possible plutonium Frenkel defect combination formed in PuO_2 under the condition of O-rich and O-deficient.

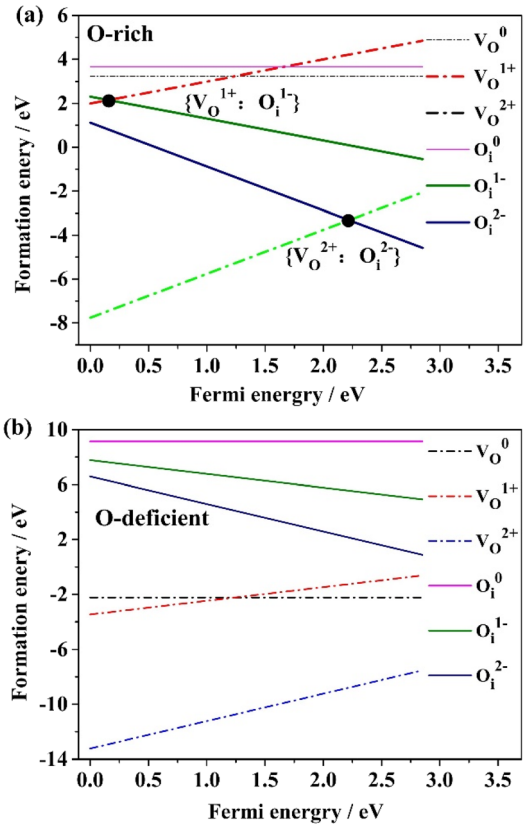

Fig. 7 Formation energies of oxygen vacancies in various charge states within whole E_F level, and possible oxygen Frenkel defect combination formed in PuO_2 under the condition of O-rich and O-deficient.

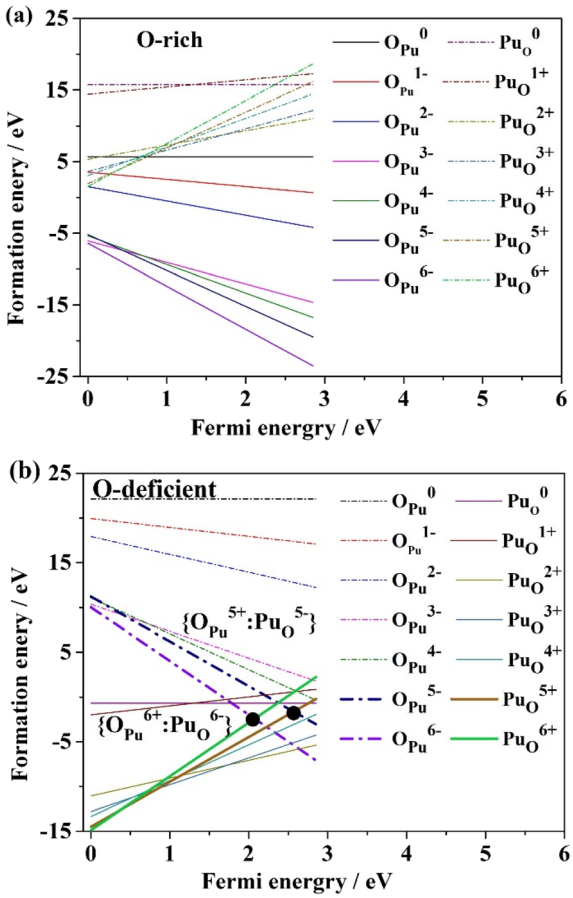

Fig. 8 ForFimation energies of antisite atoms in various charge states, and possible antisite defect combinations formed in PuO_2 under the condition of both O-rich and O-deficient.

The results suggest that the presence of an oxygen environment significantly affects the formation of both oxygen Frenkel defects and plutonium Frenkel defects. While charge states do affect the formation energy of plutonium Frenkel defects, this effect is relatively minor compared to that of oxygen Frenkel defects. These findings are consistent with earlier research on PuO_2.[21,26]

3.4 Antisite pairs

The formation energies of the antisite pair were computed under both O-rich and O-deficient conditions, as illustrated in Fig. 8. Conventionally, an antisite pair cannot be formed. In Fig. 8, it is observed that the antisite atom O_{Pu} is unable to form under O-rich conditions, whereas Pu_O readily forms under O-deficient conditions. The formation energies for the two antisite pairs {O_{Pu}^{5+}: Pu_O^{5-}} and {O_{Pu}^{6+}: Pu_O^{6-}} under O-deficient conditions are −1.58 eV and −2.26 eV, respectively. The negligible difference (<1 eV) between the formation energy of these two types of antisite pairs implies that both of them dominate as defects, providing a new insight into antisite pairs under O-deficient conditions. This outcome indicates that the oxygen environment exerts a significant influence on antisite pairs' formation. However, the charged states' effect on the antisite pair's formation energy is comparatively minor.

4 Conclusions

In summary, we have systematically investigated the process of intrinsic point defects including vacancies, interstitials, and particularly antisite atoms in PuO_2 by the first-principles plane-wave pseudopotential calculations. The whole charge state of these point defects and the effect of oxygen partial pressure are considered.

For the individual point defects, the most stable charge state varies with the Fermi energy E_F and oxygen environment. Under O-rich condition, V_{Pu}^{4-} is the most stable near the top of valence band, while O_{Pu}^{6-} is the most stable near the bottom of conduction band. In O-deficient environment, the most stable charge states in both cases change to Pu_O^{6+} and V_{Pu}^{4-}, respectively. It is surprising to find that the antisite atoms O_{Pu} and Pu_O dominate the behaviour of point defect in PuO_2.

Schottky defects can take three possible forms, *i.e.*, {$2V_{Pu}^{3-}$: $3V_O^{2+}$}, {V_{Pu}^{4-}: $2V_O^{2+}$}, and {$2V_{Pu}^{1-}$: V_O^{2+}}, under O-rich condition with {$2V_{Pu}^{3-}$: $3V_O^{2+}$} being the most stable. Under O-deficient condition, Schottky defects can take two forms, {$4V_O^{1+}$: V_{Pu}^{4+}} and {$3V_O^{1+}$: V_{Pu}^{3-}} with the latter being more stable.

Cation Frenkel defects can occur in two forms $\{V_{Pu}^{3-}: Pu_i^{3+}\}$ and $\{V_{Pu}^{4+}: Pu_i^{4+}\}$ under the O-deficient condition, with the latter being more stable. Anion Frenkel defects can occur in two forms $\{V_O^{+}: O_i^{-}\}$ and $\{V_O^{2+}: O_i^{2-}\}$ under O-rich condition, with the latter being more stable.

Two types of antisite pairs were found to be possible under O-deficient conditions, $\{O_{Pu}^{5-}: Pu_O^{5+}\}$ and $\{O_{Pu}^{6-}: Pu_O^{6+}\}$, with the latter being more stable.

Overall, our results demonstrate that the charge states and existing forms of the intrinsic point defect processes strongly depend on the oxygen condition. From the energetics of the defects, the relative stability ranked in order of rising sequence of formation energies: Schottky defects > cation Frenkel > anion Frenkel > antisite pair. This indicates that the dominant defects in PuO_2 are Schottky defects, being consistent with the experiment.[8,10]

Conflicts of interest

There are no conflicts to declare.

Acknowledgements

This work is supported by the National Natural Science Foundation of China (No. 21601167 and 22176181) and the Foundation of President of China Academy of Engineering Physics (Grant No. YZJJZQ2022011).

References

1 B. Sun, H. Liu, H. Song, G. Zhang, H. Zheng, X. Zhao and P. Zhang, *Phys. Lett. A*, 2012, **376**, 2672–2676.
2 H. Yu, D. Meng, H. Huang and G. Li, *J. Nucl. Mater.*, 2014, **452**, 6–9.
3 K. Moore and G. van der Laan, *Rev. Mod. Phys.*, 2009, **81**, 235–298.
4 M. Freyss, N. Vergnet and T. Petit, *J. Nucl. Mater.*, 2006, **352**, 144–150.
5 M. Cooper, M. Rushton and R. Grimes, *J. Phys.: Condens. Matter*, 2014, **26**, 105401.
6 J. Haschke and T. Ricketts. *Los Alamos Tech. Rep.*, 1995, LA-12999-MS.
7 X. Tian, T. Gao, C. Lu, J. Shang and H. Xiao, *Eur. Phys. J. B*, 2013, **86**, 1–7.
8 Y. Lu, Y. Yang and P. Zhang, *J. Alloys Compd.*, 2015, **649**, 544–552.
9 C. Guéneau, N. Dupin, B. Sundman, C. Martial, J. Dumas, S. Gossé, S. Chatain, F. De Bruycker, D. Manara and R. Konigs, *J. Nucl. Mater.*, 2011, **419**, 145–167.
10 C. Guéneau, A. Chartier, P. Fossati, L. Brutzel and P. Martin, *Compr. Nucl. Mater.*, 2012, **2**, 21–59.
11 B. Dorado and P. Garcia, *Phys. Rev. B: Condens. Matter Mater. Phys.*, 2013, **87**, 195139.
12 M. Freyss and T. Petit, *International Conference of Computational Methods in Sciences and Engineering* 2004 (ICCMSE 2004).
13 L. Zhang, B. Sun, Q. Zhang, H. Liu, K. Liu and H. Song, *Appl. Surf. Sci.*, 2020, **516**, 146164.
14 M. Kato, T. Uchida and T. Sunaoshi, *Phys. Status Solidi C*, 2013, **10**, 189–192.
15 B. Ao, R. Qiu, H. Lu, X. Ye, P. Shi, P. Chen and X. Wang, *J. Phys. Chem. C*, 2015, **119**, 101–108.
16 X. Wen, R. Martin, T. Henderson and G. Scuseria, *Chem. Rev.*, 2012, **113**, 1063–1096.
17 S. Dudarev, G. Botton, S. Savrasov, C. Humphreys and A. Sutton, *Phys. Rev. B: Condens. Matter Mater. Phys.*, 1998, **57**, 1505–1509.
18 X. Xiang, G. Zhang, X. Wang, T. Tang and Y. Shi, *Phys. Chem. Chem. Phys.*, 2015, **17**, 29134–29141.
19 S. Zhang, S. Wei and A. Zunger, *Phys. Rev. B: Condens. Matter Mater. Phys.*, 2001, **63**, 075205.
20 T. Mccleskey, E. Bauer, Q. Jia, A. Burrell, B. Scott, S. Condradson, A. Mueller, L. Roy, X. Wen, G. Scuseria and R. Martin, *J. Appl. Phys.*, 2013, **113**, 013515.
21 P. Tiwary, A. van de Walle, B. Jeon and N. Grønbech-Jensen, *Phys. Rev. B: Condens. Matter Mater. Phys.*, 2011, **83**, 1126–1129.
22 L. Petit L, A. Svane, Z. Szotek, W. Temmerman and G. Stocks, *Phys. Rev. B: Condens. Matter Mater. Phys.*, 2010, **81**, 045108.
23 K. Matsunaga, T. Tanaka, T. Yamamoto and Y. Ikuhara, *Phys. Rev. B: Condens. Matter Mater. Phys.*, 2003, **68**, 085110.
24 K. Reuter and M. Scheffler, *Phys. Rev. B: Condens. Matter Mater. Phys.*, 2002, **65**, 035406.
25 M. Chase, *NIST-JANAF Thermochemical Tables*, American Institute of Physics, 1998, 4th edn.
26 M. Qin, M. Cooper, E. Kuo, M. Rushton, R. Grimes, G. Lumpkin and S. Middleburgh, *J. Phys.: Condens. Matter*, 2014, **26**, 495401.